

# Determination of Cross Section for Different Fusion Reactions in Terms of Lattice Effects in Solid State Internal Conversion for Different metallic Crystalline Environments

## Abstract

*In present paper, the cross section for  $D(d,p)T$ ,  $D(d,\gamma)^4\text{He}$ ,  $T(d,n)^4\text{He}$  and  $D(p,\gamma)^3\text{He}$  fusion reactions in terms of the lattice effect in solid state internal conversion for different structures and different metallic crystalline environments in comparison with palladium environment has been determined. Elements that we used in this article are Ni, Ru, Rh, Pt, Ta, Ti, Zr, which are contained FCC, BCC and HCP lattice structures. Fusionable particles are solved as a sublattice in mentioned crystalline metals. Fusion reactions are generated by flux of incoming fusionable particles. We took lattice effect part into our calculations with regarding the Bloch function for the initial and final state of three body system. Three body system involved the host lattice, sublattice and incident particles. The cross section for performing each fusion reaction inside different metal is computed using the state of initial and final system. Then our results for cross section of different metal are compared with palladium metal. Finally, the solid state internal conversion coefficient is obtained by considering the lattice effect.*

**Key words:** internal conversion, fusion, lattice, deuterium

## 1. Introduction

Nowadays using nuclear energy is very important as a clean source of energy. There are two kinds of nuclear reactions, fusion and fission. Since fusion reaction has less radioactive radiation and the fusion fuels required for these reactions are more sufficiently available in the nature, therefore fusion reactions are important to study.

The ability of palladium to absorb hydrogen was recognized as early as the nineteenth century by Thomas Graham [1]. In the late 1920s, two Austrian born scientists, Friedrich Paneth and Kurt Peters, originally reported the transformation of hydrogen into helium by spontaneous nuclear catalysis when hydrogen was absorbed by finely divided palladium at room temperature [1,2]. In 1927, Swedish scientist J. Tandberg stated that he had fused hydrogen into helium in an electrolytic cell with palladium electrodes [1]. On the basis of his work, he applied for a Swedish patent for "a method to produce helium and useful reaction energy". After deuterium was discovered in 1932, Tandberg continued his experiments with heavy water [1]. The term "cold fusion" was used as early as 1956 in a New York Times article about Luis W. Alvarez's work on muon-catalyzed fusion [4]. Jones had worked for some time on muon-catalyzed fusion, a known method of inducing nuclear fusion without high temperatures, and had written an article on the topic entitled "Cold nuclear fusion" that had been published in Scientific American in July 1987 [5]. In 1985, many years after Pons and Fleischmann separation, Fleischmann continued his researches and published many articles [5]. In 1988, Fleischmann and Pons applied to the United States Department of Energy for funding towards a larger series of experiments. Up to this point

38 they had been funding their experiments using a small device built with \$100,000 out-of-pocket  
39 [5]. In 1989, Fleischmann and Pons published the result of their experiments which showed the  
40 approval of the cold fusion in several papers. [6] (Other scientists' works were also published  
41 [7]). In 1989, observations of Stanley Pons and Martin Fleischmann about fusion in room  
42 temperature gained a lot of attention [8]. After that the word "**cold fusion**" used for **low-energy**  
43 **nuclear reactions (LENR)**[9]. In September 1990 the National Cold Fusion Institute listed 92  
44 groups of researchers from 10 different countries that had reported corroborating evidence of  
45 excess heat [10]. From 1990 to 2008, special researches were done in this field in India [11]. In  
46 1991, the failure of all the experiments and researches were declared [12]. In 1 January 1991,  
47 Pons left his tenure, and both he and Fleischmann quietly left the United States [13,14]. In 1992  
48 they resumed research with Toyota Motor Corporation's IMRA lab in France [13]. Fleischmann  
49 left for England in 1995, and the contract with Pons was not renewed in 1998 after spending \$40  
50 million with no tangible results. The IMRA laboratory was closed in 1998 after spending £12  
51 million on cold fusion work. Pons has made no public declarations since, and only Fleischmann  
52 continues giving talks and publishing papers [15]. In 1995, many experimental works is done on  
53 gaseous metals for determining screening effect [16]. From 1998 to 2001, these experiments  
54 continued on metallic environments [17-19]. In 1999 the Japan C-F Research Society was  
55 established to promote the independent research into cold fusion that continued in Japan [20].  
56 The society holds annual meetings; the 12th meeting took place on December 17-18, 2011 at  
57 Kobe University [21]. In 2000, the electron screening effect on cold fusion reaction was studied  
58 for D + D in the metallic environment [9]. In 2002, they released a two-volume report, "Thermal  
59 and nuclear aspects of the Pd/D<sub>2</sub>O system," with a plea for funding [22]. In 2002, the  
60 enhancement of cold fusion and solid state effect were studied in deuterated metal for D+D [23].  
61 From 2002 to 2004, the screening effect on 50 metals and insulator is checked by series of  
62 experiments [24-26]. In 2003, the enhancement of deuteron-fusion reactions in metals and  
63 experimental implications were studied for electron screening effect [27]. In 2004, the subject of  
64 solid state internal conversion came up [28]. And DOE review started again [29]. In 2005, many  
65 efforts were done to make an apparatus according to the Fleischmann and Pons' works, finally,  
66 Cold fusion apparatus was made at San Diego Space and Naval Warfare Systems Center . They  
67 used other names instead of cold fusion to reduce the effect of previous failures. Often they prefer  
68 to name their field **Low Energy Nuclear Reactions (LENR)** or **Chemically Assisted Nuclear**  
69 **Reactions (CANR)**, also **Lattice Assisted Nuclear Reactions (LANR)**, **Condensed Matter**  
70 **Nuclear Science (CMNS)** and **Lattice Enabled Nuclear Reactions** [30-33].

71 In 2007, the Naval Research Laboratory published a literature review explaining why most  
72 researchers have usually been unable to replicate successful LENR experiments, saying that the  
73 loading ratio of gas to metal was the most crucial aspect, which can be affected by metal  
74 properties, cell configuration, and the experimental protocols [34]. In 2007, nuclear physicist and  
75 engineering professor Jean-Paul Biberian published an update surveying the previous 15 years of  
76 work, stating that nuclear reactions which are not predicted by current theories have been proven  
77 [35].

78 In 2002, Peter Kalman and Thomas Keszthelyi studied this problem on different metals.  
79 They studied many different factors to explain the enhancement of cross section. For example,  
80 the electron screening was checked for 29 deuterated metals and 5 deuterated  
81 insulators/semiconductors from periodic tables. Among them, metals were most convenient.  
82 Some of the other factors that they considered were: stopping power, thermal motion,  
83 channeling, diffusion, conductivity, and crystal structure and electron configuration. None of  
84 them could explain the observed enhanced cross section [23, 25, 27, 36-38]. In 2004, they found  
85 a reason to explain the enhancement of cross section that was called solid state internal  
86 conversion [28]. In 2008, screening effect is studied for the first time on metals by considering  
87 solid state; actually solid state of metals is expressed in experiments [39]. Finally, in 2009, they  
88 considered a metal with its lattice structure and entered the lattice shape of the solid in their  
89 internal conversion calculations [40]. Their calculations were just for  $D(p,\gamma)^3\text{He}$  reaction.

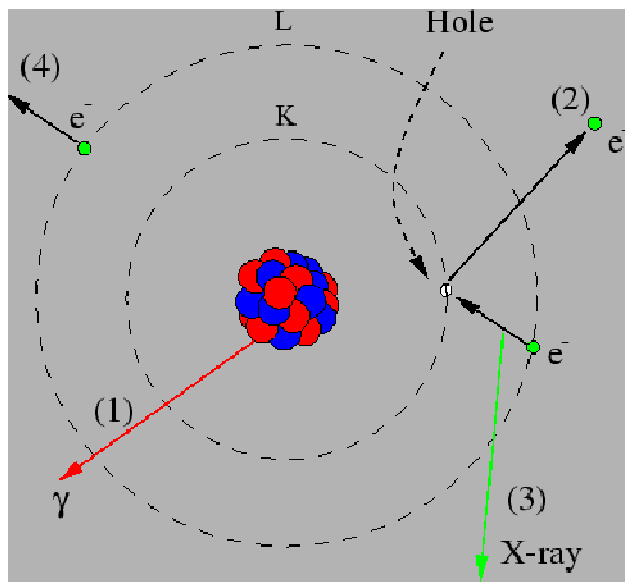
90 Here different metals are considered. We choose such metals that are shown the best results  
91 in term of screening effect and the density of deuterium [41]. In this article, for comparing  
92 internal conversion and lattice effect in solid state internal conversion, we calculate cross section  
93 for different seven particles in plus palladium for  $D(p,\gamma)^3\text{He}$ ,  $D(d,p)\text{T}$ ,  $D(d,\gamma)^4\text{He}$ ,  $\text{T}(d,n)^4\text{He}$ .

94 The aim of this work is determination of fusion cross section for different reactions in different  
95 metallic environments regarding the lattice effect in solid state internal conversion (LEISSIC).  
96 For approaching to this aim we studied on the different steps that are followed by: in the first  
97 step right after introduction, the aspects of IC, SSIC and LEISSIC are explained. In second step,  
98 different special lattice such as FCC, BCC and HCP are introduced in details. In third step,  
99 LEISSIC and other required quantities for determining FCS and LEISSIC coefficient for Pd  
100 environment are computed. In fourth step, all calculations in the previous step are repeated for  
101 Ni, Ru, Rh, Pt, Ta, Ti, Zr. In fifth step, microscopic FCS for all elements are determined in  
102 different reaction for element host particle. Finally, in the sixth step, we can suggest the best kind  
103 of lattice, fusion reaction and metallic environment which have high value LEISSIC when cold  
104 fusion happening.

## 105 **2. Internal Conversion (IC) and Solid State Internal Conversion (SSIC)**

106 **Internal conversion** is a radioactive decay process where an excited nucleus interacts with  
107 an electron in one of the lower atomic orbitals, causing the electron to be emitted from the atom.  
108 Thus, in an internal conversion process, a high-energy electron is emitted from the radioactive  
109 atom, but without beta decay taking place. For this reason, the high-speed electrons from internal  
110 conversion are not beta particles ( $\beta$  particles), since the latter come from beta decay. Since no  
111 beta decay takes place in internal conversion, the element atomic number does not change, and  
112 thus (as is the case with gamma decay) no transmutation of one element to another is seen. Also,  
113 no neutrino is emitted in internal conversion.

114 Internally converted electrons do not have the characteristic energetically-spread spectrum of  
115  $\beta$  particles, which results from varying amounts of decay-energy being carried off by the  
116 neutrino (or antineutrino) in beta decay. Internally converted electrons, which carry a fixed  
117 fraction of the characteristic decay energy, have a well-specified discrete energy. The energy  
118 spectrum of a  $\beta$  particle is thus a broad hump, extending to a maximum decay energy value,  
119 while the spectrum of internally converted electrons is a sharp peak.



120

121

Figure 1: Internal conversion

122 In the internal conversion process, the wave function of an inner shell electron penetrates the  
123 nucleus (i.e. there is a finite probability of the electron in an s-atomic orbital being found in the  
124 nucleus) and when this is the case, the electron may couple to the excited state and take the  
125 energy of the nuclear transition directly, without an intermediate gamma ray being produced  
126 first.

127 Most internal conversion electrons come from the K shell (1s state, see electron shell), as  
128 these two electrons have the highest probability of being found inside the nucleus. After the  
129 electron has been emitted, the atom is left with a vacancy in one of the inner electron shells. This  
130 hole will be filled with an electron from one of the higher shells and subsequently a characteristic  
131 x-ray or Auger electron will be emitted [9].

132 Scientists first examined different environments; among them, the deuterated metallic  
133 environments were the best to be a host environment for cold fusion. At first they studied the  
134 gaseous metals, and then they considered the target as a solid. Comparing the results of these  
135 experiments with the results obtained with gaseous targets extra fusion events were obtained. The  
136 enhancement in the fusion rate is attributed to the presence of solid state material but up till now the  
137 theoretical explanation of the phenomenon is still missing [42-44]. In what follows we suggest a possible  
138 mechanism called solid state internal conversion process that should be considered when trying to  
139 understand the extra fusion events. In “ordinary” nuclear physics the internal conversion process is a well-

140 known reaction in which a nuclear isomer loses its nuclear excitation energy by ejecting an electron of its  
141 Surroundings (one of the atomic electrons) instead of by emitting radiation [45].

142  
143 Internal conversion process arises due to the electromagnetic interaction between the nucleon  
144 and the electronic shell. A similar process can take place in a solid between fusionable nuclei and any  
145 charged particle in the crystal. The solid state internal conversion process counterparts of the  $D(p,\gamma)^3\text{He}$   
146 nuclear reaction -can be processes consisting of (a) a bound-free electron transition  $p + d + (e) \rightarrow ^3\text{He} +$   
147  $e$  and (b) a bound-free deuteron transition  $p + d + (d) \rightarrow ^3\text{He} + d$ . Therefore, as internal conversion  
148 happened in solid environment in addition of electron channel we have deuterium channel too  
149 [28].

150 We understood that in a solid (deuterated Pd) the interchange of light phonon results in an  
151 absorbent potential between semi-free fusionable particles( between semi-free deuterium).  
152 Absorption increases by relative increase of deuterium in the host material and may have eye  
153 catching effect on nuclear fusion rate in low temperature that is basically determined by strong  
154 colony repulsion. It is shown that in a solid material, nuclear fusion reactions can happen in  
155 solid state internal conversion that creates transit for every charged particle by electromagnetic  
156 reaction [28].

### 157 **3. Describing mentioned lattice in this article: FCC, BCC, HCP**

158  
159 In this article, these elements are studied: Ni, Ru, Rh, Pt, Ta, Ti, Zr. Which, Ni, Pt, Rh have a  
160 FCC lattice such as Pd. Ru, Ti, Zr have a hexagonal lattice and the lattice of Ta is BCC.

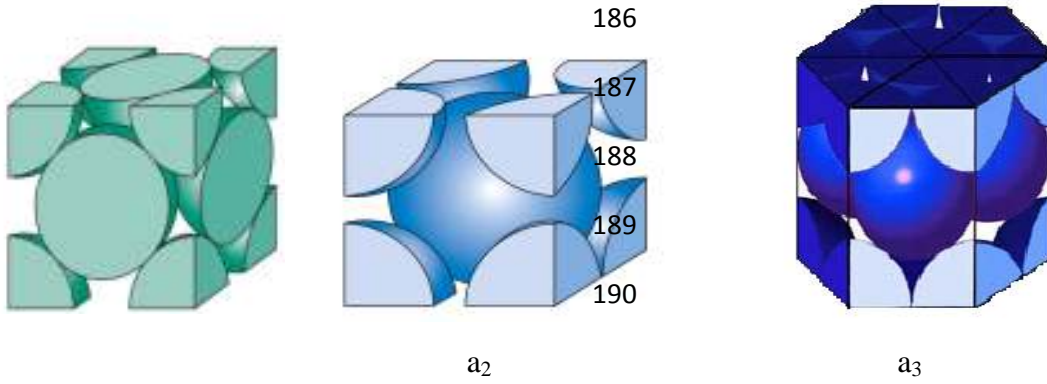
161 After investigating prior experimental work, finally in 2008 solids are considered without  
162 their lattice crystal [39]. Then, in 2009 calculations are continued for Pd and with regarding the  
163 crystalline lattice [40]. Before study on solid state internal conversion the scientists examined  
164 screening effect on metals to finding the reasons of the enhancement FCS of metals which was  
165 observed[41].In this article chosen element are significant in screening effect or deuterium  
166 density. For example, Ti and Zr showed the most screening potential in the experiments [27]. Ta  
167 and Zr had the most solved deuterium density [41]. Whereas having a maximum deuterium  
168 density in Ti depends on having high temperature [28].

169 The most important quantities that change during calculations are unit cell volume and the  
170 number of atom that belongs to each kind of lattice. Those quantities are explained for each  
171 lattice that is following.

172 In each unit cell of FCC and BCC lattice, eight atoms stand on the corner of cubic that are  
173 collaborative between eight other closed cubic (Fig 2,  $a_1$  and  $a_2$ ),thus, each unit cell has one atom  
174 from corners ( $8 \times \frac{1}{8} = 1$ ). For FCC there is one atom which belongs to two closed cubic but for  
175 BCC one atom locates in the center of each unit cell. So, FCC and BCC lattice have respectively  
176 3 atoms from all 6 sites ( $6 \times \frac{1}{2} = 3$ ) and one atom from its center. Therefore, FCC and BCC  
177 have four( $1 + 3 = 4$ ) and two ( $1 + 1 = 2$ ) atoms for each unit cell respectively.

178 HCP lattice: In each unit cell of HCP (see fig.2,a<sub>3</sub>), there are two atoms on the top and down sides that  
 179 are shared between two closed unit cells ( $2 \times \frac{1}{2} = 1$ ), on the other sides of the unit cell there are six  
 180 atoms. Each atom belong two closed unit cells ( $6 \times \frac{1}{2} = 3$ ). There are twelve atoms in the corners  
 181 that are collaborating between three closed unit cells ( $12 \times \frac{1}{3} = 4$ ). Consequently, there are eight  
 182 atoms that are completely belonging to one unit cell. In this lattice there are two lattice constants:  
 183 c height of unit cell and a, the face of hexagonal.

184



190 a<sub>1</sub>

a<sub>2</sub>

a<sub>3</sub>

191 *Figure 2: Shape of unit cell; a<sub>1</sub>: FCC unit cell, a<sub>2</sub>: BCC unit cell, a<sub>3</sub>:HCP unit cell.*

192 The volume of unit cell for each lattice is defined,

$$v_{cell} = \left\{ \begin{array}{l} \frac{a^3}{4} \quad FCC \\ \frac{a^3}{2} \quad BCC \\ \frac{3\sqrt{3}}{16} a^2 c \quad HCP \end{array} \right\}, (a, c: lattice constant) \quad (31)$$

193

194

## 195 4. Lattice Effect in Solid State Internal Conversion

### 196 4.1. Cross section theory of LEISSIC

197 Since particles in the crystal are placed in specific sites, we can estimate fusion cross section  
 198 (FCS) reactions using Block theorem for describing initial and final states of this system  
 199 (palladium environment). In all formulas subscripts 1, 2 and 3 are respectively pointed at  
 200 incoming, sublattice and host particles. Also, the state of particles in the lattice is determined by  
 201 Block function [47]

$$202 \varphi_{k_3,i}(r_3) = \frac{1}{\sqrt{N}} \sum_{l_s} e^{ik_3,i \cdot l_s} a_3(r_3 - l_s - u_3(l_s))(1)$$

203 where,  $r_3$ ,  $k_{3,1}$  and  $a_3$  are respectively introduced host-particle coordinate, a wave vector of the first  
 204 Brillouan zone of the reciprocal lattice, and Wannier function. Here, Pd (palladium), d (duetron)  
 205 and e (electron) are considered as host particles. Lattice site and the displacement of the atom  
 206 located at lattice site are symbols to represent  $l_s$  and  $u_3(l_s)$ . Here N is the number of lattice  
 207 point. The sublattice particle also is described by Block function (Eq 2). Lattice contains  $N_2$   
 208 fusionable particles, for palladium system it is assumed that  $N_2 = N$ .

$$209 \quad \varphi_{k_{2,i}}(r_2) = \frac{1}{\sqrt{N_2}} \sum_{l_s} e^{ik_{2,i} \cdot l_s} a_2(r_2 - l_s - u_2(l_s)) \quad (2)$$

210 Here,  $a_2$  and  $a_3$  are Wannier functions for sublattice and host particles respectively that are  
 211 determined by equation 3[]

$$a_j(x) = \left( \frac{\beta_j^2}{\pi} \right)^{3/4} e^{-\frac{\beta_j^2}{2} x^2} \quad (x = r_2 - l_s), j = 2,3 \quad (3)$$

212 In the above formula,  $\beta_j = \sqrt{m_j \omega_j / \hbar}$  [22]. The initial state  $\Psi_i$  for the three particles that  
 213 participate in solid state assisted fusion reaction is described by,

$$214 \quad \Psi_i = \varphi_{k_{2,i}}(r_2) \varphi_{k_{3,i}}(r_3) \varphi_1(r_1 - r_2) \quad (4)$$

215 where,  $\varphi_1(r_1 - r_2)$  is the Coulomb wave function corresponding to the state of a sublattice and  
 216 incoming particle. The Coulomb wave function is[],

$$\varphi_1(r_1 - r_2) = e^{ik_1 \cdot (r_1 - r_2)} \frac{f(k_1, r_1 - r_2)}{\sqrt{V}} \quad (5)$$

217 V is the volume of normalization,  $k_1$  is the wave vector,  $r_1$  is the coordinate of incoming particle,  
 218 and  $f$  function is defined as the following:

219  $f(k_1, x) = e^{-\pi\eta/2} \Gamma(1 + i\eta) {}_1F_1(-i\eta, 1; i[k_1 x - \mathbf{k}_1 \cdot \mathbf{x}]) (6)$   ${}_1F_1$  is the confluent hyper geometric  
 220 function [19].  $\eta$  is determined by using the eq. 7 and 8 [46].

$$\eta = 0.1575 z_1 z_2 \left( \frac{A}{E} \right)^{1/2} \quad (7)$$

$$A = \frac{A_1 A_2}{A_1 + A_2} \quad (amu) \quad (8)$$

221 Where  $z_1$  and  $z_2$  are the charge number of particles 1 and 2 and E is the energy of incoming  
 222 particle.  $A_1$  and  $A_2$  are the mass of incident and sublattice particles that are measured in amu unit.  
 223 The final state of this three- body system is defined by,

$$224 \quad \Psi_f = \psi_f(r_1, r_2) \varphi_f(r_3) F_{cb}(z_3, z_{12}, v_{3,12}) \quad (9)$$

225 Where  $\varphi_f$  is a plane wave of wave vector  $k_3$  that is corresponded to an outgoing particle 3.

$$\varphi_f(r_3) = \frac{1}{\sqrt{V}} e^{ik_3 \cdot r_3} \quad (12)$$

226  $\psi_f$  stands for the outgoing fusion product leaving a deuteron lattice point vacant that is given in  
 227 the relative coordinate ( $r = r_1 - r_2$ ) and the center of mass coordinate ( $R = m_1 r_1 + m_2 r_2 / m$ ) of the  
 228 particles of the rest masses  $m_1$  and  $m_2$ , then we have

$$229 \psi_f(r, R) = \frac{1}{\sqrt{V}} e^{iK \cdot R} \chi(r) \quad (13)$$

230 Where  $K$  and  $\chi(r)$  are the wave vector of fusion product and a nuclear wave function,  
 231 respectively.

$$\chi(r) = \left( \frac{\lambda^2}{\pi} \right)^{3/4} e^{-\lambda^2 r^2 / 2} \quad (14)$$

232 We determine the Coulomb interaction between host particle and the product of the incident and  
 233 sublattice reaction using the Fermi correction;

$$234 F_{Cb} = \sqrt{2\pi\xi} \frac{e^{-\pi\xi}}{\sqrt{1-e^{-2\pi\xi}}} \quad (15)$$

235 Where,  $\xi = z_3 z_{12} \alpha_f \sqrt{\mu c^2 / 2Q}$  and  $\alpha_f$  is the fine structure constant.  $\mu$  is the reduced mass

$$\mu = \frac{(m_1 + m_2) m_3}{m_1 + m_2 + m_3} \quad (16)$$

236 the element of s-matrix that is used for determining of the cross section of the different fusion  
 237 reaction is known as,

$$238 S_{fi} = \frac{2\pi}{i\hbar} \iiint \Psi_f^* \frac{z_1 z_3 e^2}{|r_1 - r_3|} \Psi_i d^3 r_1 d^3 r_2 d^3 r_3 \delta(E/\hbar) \quad (17)$$

239 With a little simplification on this integral and using the Hatree-Fok approximation for Coulomb  
 240 interaction part of integral, we have

$$241 \frac{z_1 z_3 e^2}{|r_1 - r_3|} = \frac{z_1 z_3 e^2}{2\pi^2} \int d^3 q \frac{1}{q^2} e^{iq \cdot (r_1 - r_2)} \quad (18)$$

242 Putting the Fourier transform of Eq.13 in Eq.16, and applying the approximation 17 and  
 243 comparing it with  $\langle \sigma v \rangle$  formula, the cross section of fusion reaction between host and target  
 244 fusible particles is obtained as the following,

$$\begin{aligned} & \sigma_2 \\ & = C_0 \frac{\exp(-2\pi\eta)}{E} \end{aligned} \quad (19)$$

245  $E$  is the energy of incoming particle and  $C_0$  is determined by,

$$246 C_0 = |F_{Cb}|^2 A_0 k_\mu \left( \frac{\beta_2}{K_Q} \right)^3 \langle |\tilde{\chi}|_{K=K_Q}^2 \rangle_{\Omega_K} \quad (20)$$

247 With  $\Omega_K$  denoting the solid angle in the  $K$  space,  $\beta_2 = \sqrt{m_d \omega / \hbar}$ ,  $A_0 = 128 \alpha_f^3 z_1^3 z_3^2 z_2 m_1 c^2 \sqrt{\pi}$ ,  
 248  $K_Q = \sqrt{2\mu c^2 Q} / (\hbar c)$ ,  $Q$  is the energy of the reaction,  $k_\mu = \mu c / \hbar$ .

249 the average of nuclear wave function is defined by,

$$\langle |\tilde{\chi}|_{K=K_0}^2 \rangle_{\Omega_K} = \left| \tilde{\chi} \left( \frac{m_2}{m} K \right) \right|^2 = \frac{8\pi^{3/2}}{\lambda^3} e^{-\frac{4K^2}{9\lambda^2}} \quad (21)$$

250  $m_n$ , nucleons mass,  $\omega_n$  angular frequent of binding energy are calculated for each reaction  
 251 separately (table 4).

$$\lambda = \frac{\sqrt{m_n \omega_n}}{\hbar} \quad (22)$$

$$m_n = m_i + m_{He}, i = d \text{ or } t \quad (23)$$

$$\omega_n = \frac{\text{binding energy of He(MeV)}}{\hbar} \quad (24)$$

252 Here,  $C_0$  is calculated for one d or one Pd. In order to compare  $C_0$  with astrophysical factor ( $S(0)$ ) in  
 253 ordinary state, it must be calculated considering the density of these particles. So, we use the  
 254 Eq.24

$$NC_0 = A\Delta R_h C_1 \quad (25)$$

255 In this case, N is defined by,

$$N(Pd) = V_{eff}/v_{cell} \quad (26)$$

256 Where  $v_{cell} = d^3/4$ ,  $V_{eff} = A\Delta R_h$  and  $d = 3.89 \times 10^{-8} cm$  is the lattice constant

$$N(d) = u V_{eff}/v_{cell} \quad (27)$$

257 In Eq.23, u is the ratio of deuteron to palladium number density. For electron  $u = 10$  which is the  
 258 number of electron valence in palladium.  $C_0$  contains all the properties of the lattice. For  
 259 comparison the fusion cross section with and without LEISSIC we have to determine the  
 260 macroscopic cross section.

$$261 \Sigma = N\sigma_2 \quad (28)$$

## 262 4.2. Results of numerical calculations for each reaction

263 There are two tables for all reactions that can aid in plotting the cross section and comparing  
 264 with the ordinary state. The suppositions of host, sublattice and incoming particles are expressed  
 265 for all reactions in this way: the host particles are Pd,d,e for Palladium. The sublattice is  
 266 deuterium for all reactions. The incoming particles are proton (p) in  $D(p,\gamma)^3He$ , deuterium (d) in  
 267  $D(d,p)T$  and  $D(d,\gamma)^4He$  and tritium (t) in  $T(d,n)^4He$ . Our calculation for obtaining the cross  
 268 section for all three kind of host particles are accomplished by using equations: 13,14,18,20 and  
 269 our obtained results are given in tables 1 and 2.

270

271

272

273

274

275

276

277

278  
279  
280

Table 1: our numerical calculation of necessary quantities for obtaining  $C_0$  for all chosen reactions

Type of Reactions	host particles	$A_0$ (MeV)	$\mu(\text{gr})$	$K_Q(\text{cm}^{-1})$	$ \tilde{\chi} _{K=K_Q}^2 (\text{cm}^3)$	$\xi$
D(p, $\gamma$ )3He	Pd	175	$5.013 \times 10^{-24}$	$8.91 \times 10^{12}$	$3.95 \times 10^{-38}$	10.755
	d	0.0827	$2.005 \times 10^{-24}$	$5.64 \times 10^{12}$	$5.13 \times 10^{-38}$	0.1477
	e	0.0103	-----	$2.78 \times 10^{11}$	$6.11 \times 10^{-38}$	-560382
D(d,p)T	pd	349	$6.686 \times 10^{-24}$	$8.82 \times 10^{12}$	$3.15 \times 10^{-38}$	14.462
	d	0.165	$2.229 \times 10^{-24}$	$5.09 \times 10^{12}$	$3.97 \times 10^{-38}$	0.181
	e	0.021	-----	$2.05 \times 10^{11}$	$4.45 \times 10^{-38}$	-0.0011
D(d, $\gamma$ )4He	Pd	349	$6.686 \times 10^{-24}$	$7.93 \times 10^{12}$	$3.69 \times 10^{-38}$	16.075
	d	0.165	$2.229 \times 10^{-24}$	$4.58 \times 10^{12}$	$4.51 \times 10^{-38}$	0.202
	e	0.021	-----	$1.65 \times 10^{11}$	$4.98 \times 10^{-38}$	-0.0022
T(d,n)4He	Pd	524	$8.35 \times 10^{-24}$	$2.05 \times 10^{13}$	$2.89 \times 10^{-39}$	5.863
	d	0.248	$2.387 \times 10^{-24}$	$1.10 \times 10^{13}$	$4.24 \times 10^{-39}$	0.09
	e	0.031	-----	$8.90 \times 10^{11}$	$4.30 \times 10^{-38}$	-4.228

281

282 From the results of table 1 and Eqs.18 and 28 for different reactions and host particle, we can  
283 calculate the required parameters such as  $C_0$  and  $C_1$  which are important for estimating cross  
284 section of the fusion reactions.

285

Table 2: our numerical calculation  $C_0$  and  $C_1$  for different host particle and different reactions

Type of Reactions	host particles	$k_\mu (\text{cm}^{-1})$	$ F_{cb} ^2$	$C_0$ (MeV b)	$C_1$ (MeV b)
D(p, $\gamma$ )3He	Pd	$1.42 \times 10^{14}$	$3.14 \times 10^{-28}$	$4.92 \times 10^{-38}$	$3.36 \times 10^{-24}$
	d	$0.57 \times 10^{14}$	0.61	$2.30 \times 10^{-13}$	$u \times 15.6$
	e	-----	1	$9.10 \times 10^{-13}$	$6.18 \times 10^2$
D(d,p)T	Pd	$1.90 \times 10^{14}$	$3.27 \times 10^{-38}$	$1.11 \times 10^{-47}$	$7.53 \times 10^{-34}$
	d	$0.63 \times 10^{14}$	0.5371	$1.88 \times 10^{-13}$	$u \times 12.78$
	e	-----	1	$2.48 \times 10^{-12}$	$1.687 \times 10^3$
D(d, $\gamma$ )4He	Pd	$1.90 \times 10^{14}$	$7.02 \times 10^{-41}$	$3.83 \times 10^{-50}$	$0.26 \times 10^{-35}$
	d	$0.63 \times 10^{14}$	0.4964	$2.70 \times 10^{-13}$	$u \times 18.35$
	e	-----	1	$4.31 \times 10^{-36}$	$2.93 \times 10^{-21}$
T(d,n)4He	Pd	$2.37 \times 10^{14}$	$4.44 \times 10^{-15}$	$2.05 \times 10^{-25}$	$1.39 \times 10^{-12}$
	d	$0.68 \times 10^{14}$	0.7438	$4.45 \times 10^{-15}$	$u \times 0.3024$
	e	-----	1	$1.87 \times 10^{-13}$	127.1

286

287 Since each palladium unit cell has 4 Pd atoms purely and since we suppose that the number of  
 288 host and sublattice particles are equal, then we have

$$N_{Pd} = \frac{1}{4} \times 4.22 \times 10^{22} \quad (29)$$

289 The other quantities such as,  $m_n$ ,  $\beta_2$  and  $Q$  which is mentioned before are calculated and  
 290 numerical results are summarized in table 3.

291 *Table 3: our obtaining required quantities which are calculated for determination of different fusion*

Type of Reactions	$\lambda (cm^{-1})$	$\beta_2(cm^{-1})$	Q (MeV)	Binding Energy (MeV)
D(p, $\gamma$ ) <sup>3</sup> He	$9 \times 10^{12}$	$4.81 \times 10^{14}$	5.49	7.718
D(d,p)T	$10 \times 10^{12}$	$4.81 \times 10^{14}$	4.04	8.482
D(d, $\gamma$ ) <sup>4</sup> He	$9.63 \times 10^{12}$	$4.81 \times 10^{14}$	3.27	28.3
T(d,n) <sup>4</sup> He	$21.8 \times 10^{12}$	$4.81 \times 10^{14}$	17.59	28.3

292

### 293 4.3. Calculations the solid state internal conversion coefficient for different 294 fusion reactions in Palladium crystal environment

295 With regarding to definition that exists in Ref.12, we can write  $v_{eff} = A\Delta R_h$ , where  $A$  is the  
 296 cross section of the beam,  $\Delta R_h$  is the “differential” range, that is, the distance within which the  
 297 energy of the incoming particle can be considered unchanged. The  $\Delta R_h \ll R_h$  condition helps in  
 298 an order of magnitude estimate of  $\Delta R_h$ , where  $R_h$  is the stopping range of a proton which is  
 299 about  $8 \times 10^{-2} \mu m$  at  $E = 0.01 MeV$  in Pd [20]. The quantities  $A$  and  $R_h$  were measured in  
 300  $mm^2$  and  $10^{-3} \mu m$  units. The solid state internal conversion coefficient is introduced as,

$$\alpha_{SSIC} = A\Delta R_h C_1 / S(0) \quad (30)$$

301  $S(0)$  is the astrophysical factor and the amounts of  $S(0)$  were calculated completely in the ref  
 302 44. Here since the issue is studied on the low energy (5-30 eV), the amounts of  $S(0)$  for each  
 303 reaction is a constant that are shown in table 4.

304 *Table 4: the amounts of astrophysical S-factor for different reactions in ordinary state in low energy*

Reactions	$D(p,\gamma)^3He$	$D(d,p)T$	$D(d,\gamma)^4He$	$T(d,n)^4He$
Astrophysical factor				
S(0) MeV barn	$0.2 \times 10^{-6}$	0.056	0.054	10

305

306 By using the amounts exist in tables 2, 4 and replacing them into Eq.29 the solid state internal  
 307 conversion coefficient for different reactions can be found. This coefficient indicates the internal  
 308 conversion rate in different reactions. The result of the calculations summarize in table 5.

309 *Table 5: solid state internal conversion coefficient in different reactions for e, 4d and d channels*

Reactions	$\alpha_{SSIC,d} A\Delta R_h$	$\alpha_{SSIC,e,4d} A\Delta R_h$
D(p, $\gamma$ ) <sup>3</sup> He	$u \times 7.8 \times 10^5$	$3.1 \times 10^9$
D(d,p)T	$u \times 3.03 \times 10^4$	$3.2 \times 10^6$
D(d, $\gamma$ ) <sup>4</sup> He	$u \times 3.398 \times 10^2$	$5.42 \times 10^{-20}$
T(d,n) <sup>4</sup> He	$u \times 0.03$	12.7

310

311 We find out the solid state internal conversion happens in D(p, $\gamma$ )<sup>3</sup>He and D(d,p)T reactions with  
 312 more rates. All calculations in this part are shown for palladium. In the next part we show the  
 313 results for other elements in detailed.

## 314 5. Calculations of LEISSIC for other elements

### 315 5.1. Tables of Calculation for Different Elements and Reactions

316 By using all formulas in section 3, such as what we have done for palladium, all required  
 317 quantities can be computed for mentioned elements. Because the other host particles (deuterium  
 318 and electron) don't change in these calculations and the only thing that changes is the first row of  
 319 the Table.1. Meanwhile,  $C_1$  and  $C_0$  which changes only for the elements are respectively showed  
 320 in Table 6 and 7.

321 Table 6: Our numerical calculations of  $C_0$  for different elements and reactions with FCC, BCC and HCP lattice

Quantity Elements	$C_{0,D(p,\gamma)^3He}$ (MeV barn)	$C_{0,D(d,p)T}$ (MeV barn)	$C_{0,D(d,\gamma)^4He}$ (MeV barn)	$C_{0,T(d,n)^4He}$ (MeV barn)
Pd (FCC)	$4.92 \times 10^{-38}$	$1.11 \times 10^{-47}$	$3.83 \times 10^{-50}$	$2.05 \times 10^{-25}$
Ni (FCC)	$3.44 \times 10^{-27}$	$6.79 \times 10^{-33}$	$2.56 \times 10^{-35}$	$6.98 \times 10^{-23}$
Pt (FCC)	$1.34 \times 10^{-57}$	$1.95 \times 10^{-74}$	$1.21 \times 10^{-81}$	$1.63 \times 10^{-45}$
Rh (FCC)	$1.08 \times 10^{-36}$	$7.43 \times 10^{-47}$	$6.61 \times 10^{-51}$	$1.38 \times 10^{-24}$
Ru (HCP)	$8.49 \times 10^{-37}$	$5.07 \times 10^{-46}$	$5.56 \times 10^{-50}$	$1.21 \times 10^{-30}$
Ti (HCP)	$1.10 \times 10^{-23}$	$4.63 \times 10^{-28}$	$6.49 \times 10^{-30}$	$1.93 \times 10^{-21}$
Zr (HCP)	$2.25 \times 10^{-34}$	$1.01 \times 10^{-42}$	$2.69 \times 10^{-46}$	$6.27 \times 10^{-29}$
Ta (BCC)	$1.30 \times 10^{-54}$	$3.10 \times 10^{-70}$	$5.79 \times 10^{-77}$	$2.64 \times 10^{-43}$

322

323

324

Table 7: Our numerical calculations of  $C_1$  for different elements and reactions with FCC, BCC and HCP lattice

Quantity Element		$C_{1,D(p,\gamma)3He}$ (MeV barn)	$C_{1,D(d,p)T}$ (MeV barn)	$C_{1,D(d,\gamma)4He}$ (MeV barn)	$C_{1,T(d,n)4He}$ (MeV barn)
Pd (FCC)	Pd	$3.36 \times 10^{-24}$	$7.53 \times 10^{-34}$	$0.26 \times 10^{-35}$	$1.39 \times 10^{-12}$
	d	$u \times 15.6$	$u \times 12.78$	$u \times 18.35$	$u \times 0.30$
	e	$6.18 \times 10^2$	$1.68 \times 10^3$	$2.93 \times 10^{-21}$	127.1
Ni (FCC)	Ni	$3.15 \times 10^{-13}$	$6.23 \times 10^{-19}$	$2.35 \times 10^{-21}$	$6.40 \times 10^{-9}$
	d	$u \times 21.1$	$u \times 17.25$	$u \times 24.8$	$u \times 4.08$
	e	$8.35 \times 10^2$	$2.27 \times 10^3$	$3.96 \times 10^{-21}$	$1.71 \times 10^2$
Pt (FCC)	Pt	$6.86 \times 10^{-44}$	$1.30 \times 10^{-60}$	$8.07 \times 10^{-68}$	$1.08 \times 10^{-31}$
	d	$u \times 15.27$	$u \times 12.48$	$u \times 17.93$	$u \times 2.955 \times 10^{-1}$
	e	$6.04 \times 10^2$	$1.65 \times 10^3$	$2.86 \times 10^{-21}$	$1.242 \times 10^2$
Rh (FCC)	Rh	$7.93 \times 10^{-23}$	$5.41 \times 10^{-33}$	$4.82 \times 10^{-37}$	$1.01 \times 10^{-30}$
	d	$u \times 16.76$	$u \times 13.71$	$u \times 19.68$	$u \times 3.24 \times 10^{-1}$
	e	$5.97 \times 10^2$	$1.63 \times 10^3$	$2.83 \times 10^{-21}$	122.75
Ru (HCP)	Ru	$5.20 \times 10^{-23}$	$3.10 \times 10^{-32}$	$3.40 \times 10^{-36}$	$7.41 \times 10^{-17}$
	d	$u \times 14.08$	$u \times 11.51$	$u \times 16.53$	$u \times 0.27$
	e	$4.46 \times 10^2$	$1.21 \times 10^3$	$2.11 \times 10^{-21}$	91.60
Ti (HCP)	Ti	$5.21 \times 10^{-10}$	$2.19 \times 10^{-14}$	$3.07 \times 10^{-16}$	$9.12 \times 10^{-8}$
	d	$u \times 10.86$	$u \times 8.88$	$u \times 12.76$	$u \times 0.21$
	e	172.02	469.22	$8.15 \times 10^{-22}$	$3.53 \times 10^2$
Zr (HCP)	Zr	$8.05 \times 10^{-21}$	$3.61 \times 10^{-29}$	$9.62 \times 10^{-33}$	$2.25 \times 10^{-15}$
	d	$u \times 8.24$	$u \times 6.73$	$u \times 9.67$	$u \times 16.12$
	e	$1.30 \times 10^2$	$3.55 \times 10^2$	$6.18 \times 10^{-22}$	26.80
Ta (BCC)	Ta	$7.17 \times 10^{-41}$	$1.71 \times 10^{-56}$	$3.19 \times 10^{-63}$	$1.46 \times 10^{-29}$
	d	$u \times 12.68$	$u \times 10.37$	$u \times 14.89$	$u \times 0.25$
	e	$2.51 \times 10^2$	$6.84 \times 10^2$	$1.19 \times 10^{-21}$	51.59

326

327

328 For comparing  $C_0$ , the micFCS of these metallic environments for all elements, numerical  
329 values from Table.6 can be useful. For studying the comparison of the  $C_1$  quantity see table 7.

330 According to table 7, we find out that: wherever elements themselves are considered as host  
331 particles, the results of  $C_1$  from large too small values for all reactions are: Ti, Ni, Zr, Ru, Rh, Pd,  
332 Ta and Pt. For cases that deuterium and electron are host particles, our comparing values lead to  
333 Ru, Ni, Ti, Rh, Pd, Pt, Zr, Ta and Ni, Ru, Pd, Pt, Rh, Ti, Ta, Zr respectively. In case that electron  
334 is host the number of electrons in capacity layer is too important indeed whatever the numbers of  
335 electrons increases the screening effect is enhanced. Between all reactions,  $D(p,\gamma)3He$ ,  $D(d,p)T$   
336 and  $D(d,\gamma)4He$  have larger values of  $C_1$  than  $T(d,n)4He$ .

337 (According Table.7 the result of comparing  $C_1$  for different host particles in different metallic  
338 environments are: element host particle,  $C_{1,Ti} > C_{1,Ni} > C_{1,Zr} > C_{1,Ru} > C_{1,Rh} > C_{1,Pd} > C_{1,Ta} >$   
339  $C_{1,Pt}$ ; deuterium host particle,  $C_{1,Ru} > C_{1,Ni} > C_{1,Ti} > C_{1,Rh} > C_{1,Pd} > C_{1,Pt} > C_{1,Zr} > C_{1,Ta};$   
340 electron host particle,  $C_{1,Ni} > C_{1,Ru} > C_{1,Pd} > C_{1,Pt} > C_{1,Rh} > C_{1,Ti} > C_{1,Ta} > C_{1,Zr}$ )

341

342

343

344

345

Table 8: Our numerical calculations of LEISSIC for all elements in different reactions

Quantit Elements		$\alpha_{D(p,\gamma)3He}$ $\times A\Delta R_h$	$\alpha_{D(d,p)T}$ $\times A\Delta R_h$	$\alpha_{D(d,\gamma)4He}$ $\times A\Delta R_h$	$\alpha_{T(d,n)4He}$ $\times A\Delta R_h$
Pd (FCC)	d	$u \times 7.80 \times 10^5$	$u \times 3.03 \times 10^4$	$u \times 3.40 \times 10^2$	$u \times 0.03$
	e	$3.1 \times 10^9$	$3.2 \times 10^6$	$5.42 \times 10^{-20}$	12.7
Ni (FCC)	d	$u \times 1.05 \times 10^8$	$u \times 3.08 \times 10^2$	$u \times 4.59 \times 10^2$	$u \times 0.41$
	e	$4.17 \times 10^9$	$4.07 \times 10^4$	$7.33 \times 10^{-20}$	17.15
Pt (FCC)	d	$u \times 7.63 \times 10^7$	$u \times 2.23 \times 10^2$	$u \times 3.32 \times 10^2$	$u \times 0.029$
	e	$3.02 \times 10^8$	$2.94 \times 10^4$	$5.3 \times 10^{-20}$	12.42
Rh (FCC)	d	$u \times 8.38 \times 10^7$	$u \times 2.45 \times 10^2$	$u \times 3.65 \times 10^2$	$u \times 0.032$
	e	$3.00 \times 10^9$	$2.91 \times 10^4$	0.52	12.27
Ru (HCP)	d	$u \times 7.04 \times 10^7$	$u \times 2.06 \times 10^2$	$u \times 3.06 \times 10^2$	$u \times 0.027$
	e	$2.23 \times 10^9$	$2.17 \times 10^4$	$3.91 \times 10^{-20}$	9.17
Ti (HCP)	d	$u \times 5.43 \times 10^7$	$u \times 1.59 \times 10^2$	$u \times 2.36 \times 10^2$	$u \times 0.021$
	e	$8.60 \times 10^8$	$8.38 \times 10^3$	$1.51 \times 10^{-20}$	35.37
Zr (HCP)	d	$u \times 4.12 \times 10^7$	$u \times 1.20 \times 10^2$	$u \times 1.79 \times 10^{-2}$	$u \times 1.61$
	e	$6.52 \times 10^8$	$6.35 \times 10^3$	$1.14 \times 10^{-20}$	2.68
Ta (BCC)	d	$u \times 6.34 \times 10^7$	$u \times 1.85 \times 10^2$	$u \times 2.76 \times 10^2$	$u \times 0.025$
	e	$1.25 \times 10^9$	$1.22 \times 10^4$	$2.20 \times 10^{-20}$	5.16

346

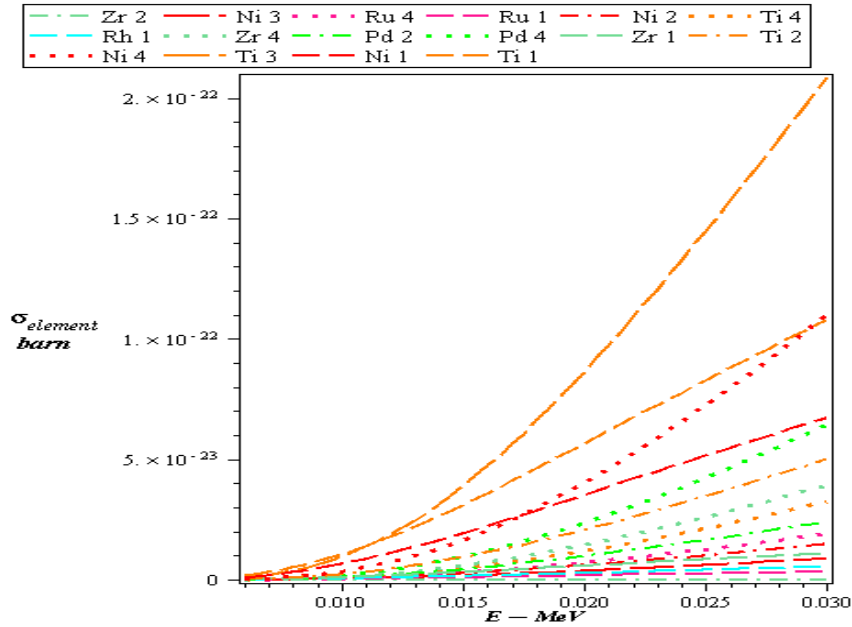
347 In the each environment IC coefficient shows internal conversion rate and determined the cross  
 348 section enhancement in each environment. By studying table 8, we find out that the internal  
 349 conversion coefficient of deuterium for D(p,γ)3He is the largest one. IC coefficient for  
 350 D(p,γ)3He for different reactions from larger to smaller value is: Ru, Ni, Rh, Pt, Zr, Ta, Ti and  
 351 Pd. As you see in this reaction Pd has the last rank. In D (d,p)T, the arrangement of the elements  
 352 is: Pd, Ru, Ni, Ti, Rh, Pt, Zr and Ta.

353 Electronic internal conversion coefficient arrangement for different elements is: Ni, Ru, Pd, Rh, Ti,  
 354 Ta, Zr, Pt. ( $\alpha_{e,Ni} > \alpha_{e,Ru} > \alpha_{e,Pd} > \alpha_{e,Rh} > \alpha_{e,Ti} > \alpha_{e,Ta} > \alpha_{e,Zr} > \alpha_{e,Pt}$ )

355 ( According to Table.8, comparing ICC values of deuterium host particle for the two largest  
 356 reactions D(p,γ)3He and D(d,p)T are respectively:  $\alpha_{d,Ru} > \alpha_{d,Ni} > \alpha_{d,Rh} > \alpha_{d,Pt} > \alpha_{d,Zr} > \alpha_{d,Ta} >$   
 357  $\alpha_{d,Ti} > \alpha_{d,Pd}$  and  $\alpha_{d,Pd} > \alpha_{d,Ru} > \alpha_{d,Ni} > \alpha_{d,Ti} > \alpha_{d,Rh} > \alpha_{d,Pt} > \alpha_{d,Zr} > \alpha_{d,Ta}$ )

### 358 6. Microscopic cross section for all elements in different reactions

359 micFCS for all metallic environment when metal is a host particle are plotted by replacing  
 360 numerical values in Table 6 and Eq.17. All FCS are divided into two groups in order to show  
 361 changes clearly: 16 maximum and 16 minimum which are respectively shown in Fig 5 and Fig 6.  
 362 Numbers 1 to 4 besides the name of the elements shows D(p,γ)3He , D(d,p)T , D(d,γ)4He and  
 363 T(d,n)4He .



364

365

Figure 5:16 maximum of micFCS in terms of incoming energy for all reactions

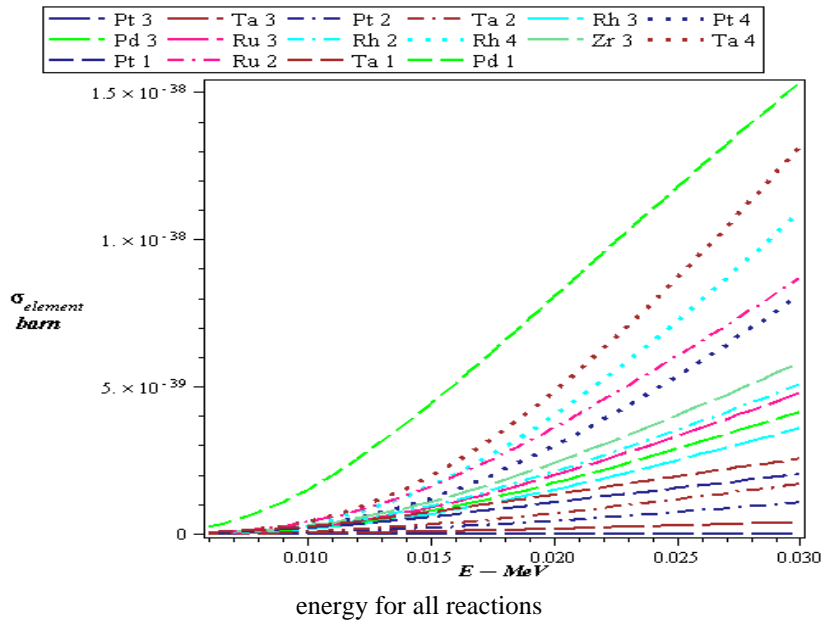
366

In the above graph, different colors shows kinds of elements and the styles of shape introduce kinds of reactions. D(p,γ)3He by “dash”, D(d,p)T by “dashdot”, D(d,γ)4He by “longdash” and T(d,n)4He by “dot” are shown. The color of Pd, Ni, Pt, Rh, Ru, Ti, Zr, and Ta are respectively: Green, red, navy, cyan, dark pink, coral, aquamarine and brown. As you see Ti and Ni have the larger cross section. After them palladium shows up just in the T(d,n)4He reaction.

368

369

370



minimum of incoming energy for all reactions

371

372

373

374

375

376

377

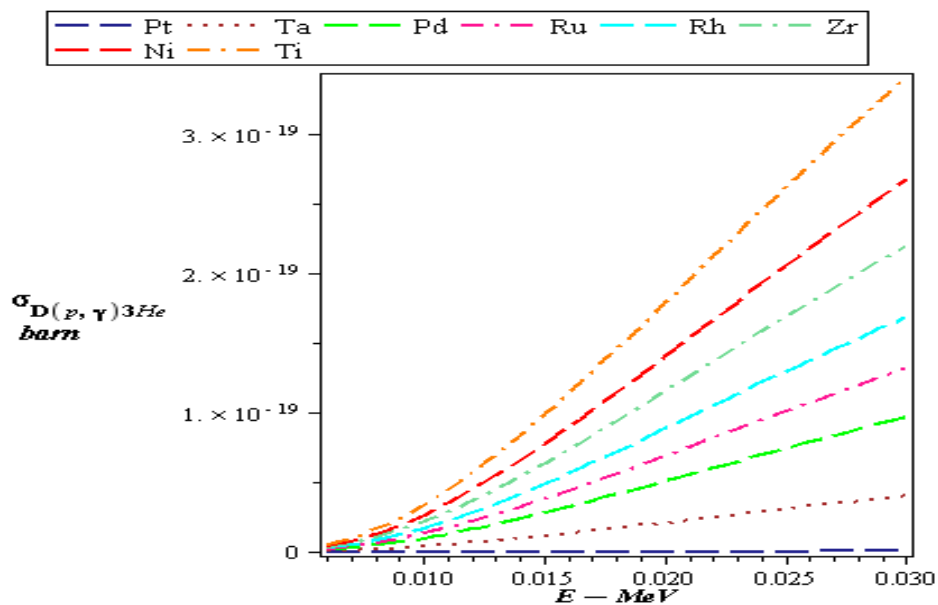
378

Figure 5:16 minimum of incoming energy for all reactions

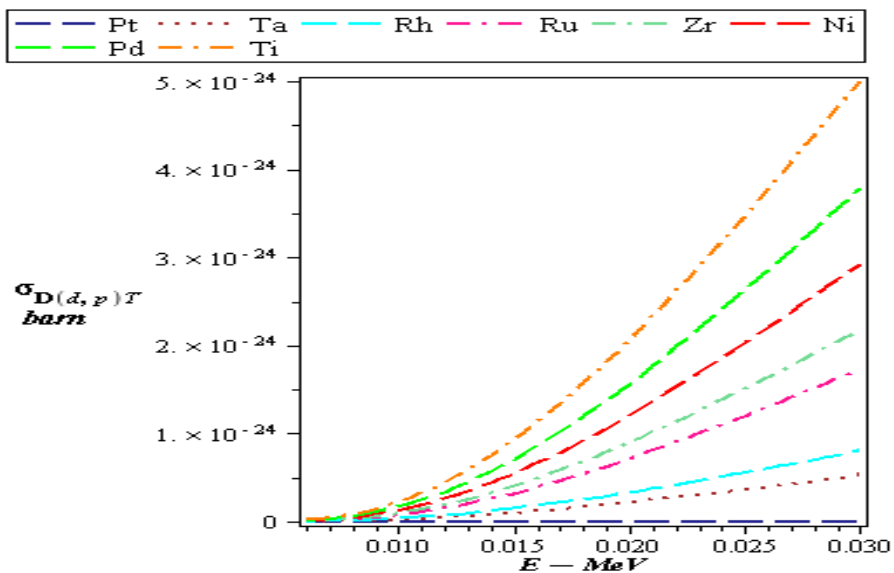
381

382

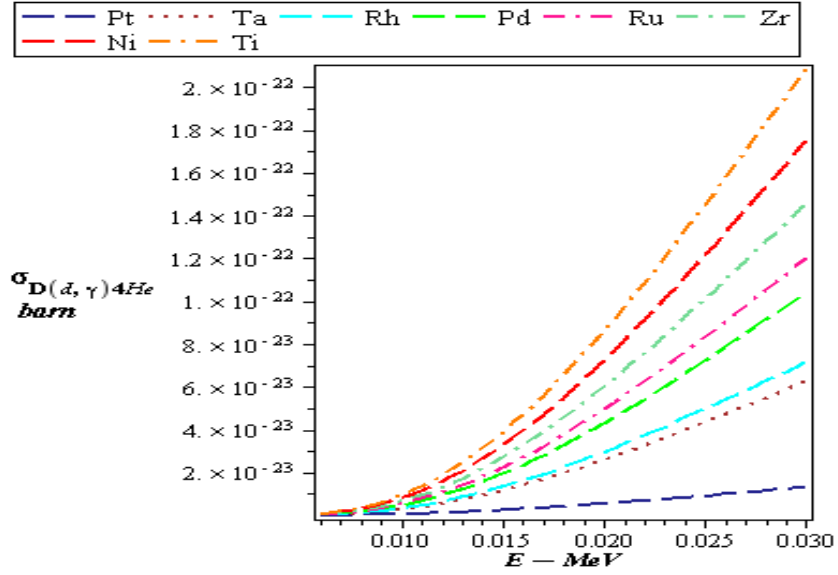
383 To realize the best kinds of lattice structure, micFCS related to element host particles are plotted  
 384 for each fusion reactions separately. Here in these graphs colors shows kinds of elements and the  
 385 styles of the graph indicate the kind of the lattice. BCC by “dot”, FCC by “long dash” and HCP  
 386 by “dashpot”.



397 Figure 7: micFCS of all elements for  $D(p,\gamma)3He$ .



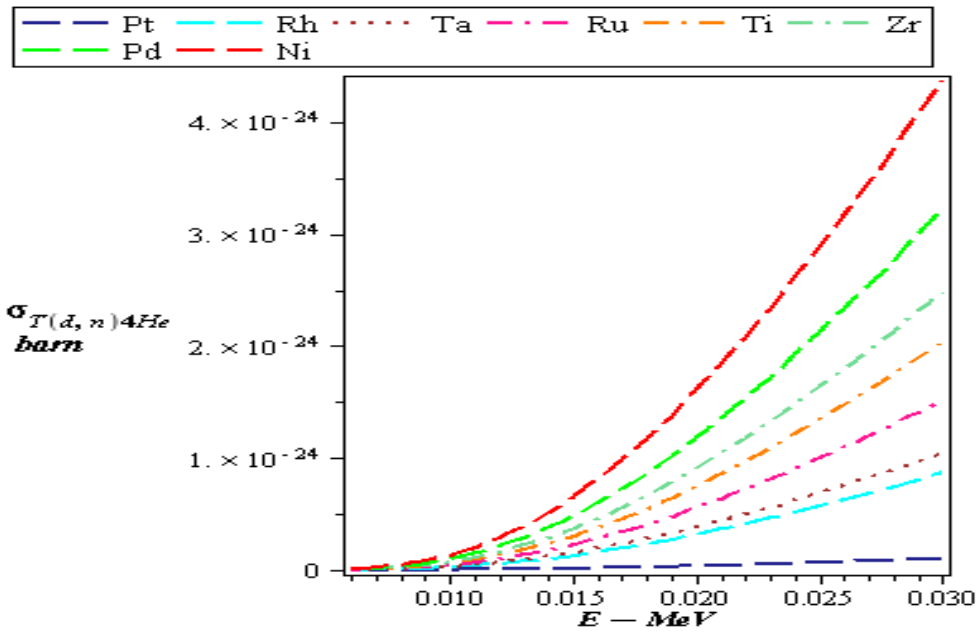
399 Figure 8: micFCS of all elements for  $D(d,p)T$



400

401

Figure 9: micFCS of all elements for D(d,γ)4He



402

403

Figure 10: micFCS of all elements for T(d,n)4He

404 For D(p,γ)3He , D(d,p)T , D(d,γ)4He (Figs. 7,8,9), Ti with HCP lattice has the largest micFCS  
 405 and Pd with FCC lattice is respectively in the sixth, second and fifth place. From Fig.10 we can  
 406 understand that Ni with FCC lattice is in the first place of micFCS and Pd is the fifth. Now the  
 407 data that are correspond to figures 7, 8, 9 and 10 are summarized in table 9.

408

409

Table 9: numerical microscopic cross sectioned values in special energy (0.025MeV) for different elements in different reactions

Quantity Element	$\sigma_{element}$ D(p, $\gamma$ ) <sup>3</sup> He (MeV)	$\sigma_{element}$ D(d,p)T (MeV)	$\sigma_{element}$ D(d, $\gamma$ ) <sup>4</sup> He (MeV)	$\sigma_{element}$ T(d,n) <sup>4</sup> He (MeV)
<b>Pd</b> <b>(FCC)</b>	$1.19 \times 10^{-38}$	$8.35 \times 10^{-49}$	$2.89 \times 10^{-51}$	$8.51 \times 10^{-28}$
<b>Ni</b> <b>(FCC)</b>	$8.19 \times 10^{-28}$	$5.12 \times 10^{-34}$	$1.93 \times 10^{-36}$	$2.89 \times 10^{-24}$
<b>Pt</b> <b>(FCC)</b>	$2.46 \times 10^{-58}$	$1.48 \times 10^{-75}$	$9.18 \times 10^{-83}$	$6.78 \times 10^{-47}$
<b>Rh</b> <b>(FCC)</b>	$2.59 \times 10^{-37}$	$5.61 \times 10^{-48}$	$5.02 \times 10^{-52}$	$5.77 \times 10^{-46}$
<b>Ru</b> <b>(HCP)</b>	$2.02 \times 10^{-37}$	$3.81 \times 10^{-47}$	$4.21 \times 10^{-51}$	$5.02 \times 10^{-32}$
<b>Ti</b> <b>(HCP)</b>	$2.62 \times 10^{-24}$	$3.50 \times 10^{-29}$	$4.93 \times 10^{-31}$	$7.97 \times 10^{-23}$
<b>Zr</b> <b>(HCP)</b>	$5.37 \times 10^{-37}$	$7.59 \times 10^{-44}$	$2.03 \times 10^{-47}$	$2.61 \times 10^{-30}$
<b>Ta</b> <b>(BCC)</b>	$3.10 \times 10^{-55}$	$2.34 \times 10^{-71}$	$4.36 \times 10^{-78}$	$1.10 \times 10^{-44}$

410

## 7. Conclusion

411

As you see, Titanium and Nickel are chosen for using them in the next options in experimental works. By studying the internal conversion coefficient, we find out that Ni and Ru might be good options. By collecting these results together we understand that the Nickel can be the best option. We can neglect Ta and the BCC lattice because of its worse results.

415

The other investigations show that: FCC and HCP lattice have a much closed results. Palladium shows good results just in the D(p, $\gamma$ )<sup>3</sup>He and D(d, $\gamma$ )<sup>4</sup>He. After Ni, the next option could be Ti.

416

## References

418

[1] US DOE 1989, p. 7.

419

[2] Paneth and Peters 1926.

420

[3] Laurence 1956.

421

[4] Kowalski 2004, II.A2

422

[5] Crease & Samios 1989, p. V1.

423

[6] Browne 1989.

424

[7] Broad 1989a.

425

[8] "60 Minutes: Once Considered Junk Science, Cold Fusion Gets A Second Look By Researchers CBS. 2009-04-17. <http://www.cbsnews.com/stories/2009/04/17/60minutes/main4952167.shtml>.

426  
427

428 [9] [www.wikipedia.com](http://www.wikipedia.com)

	[10] Mallove 1991, pp. 246–248.	429
	[11] Jayaraman 2008.	430
	[12] <i>National Cold Fusion Institute Records, 1988-1991</i> ,	431
	<a href="http://content.lib.utah.edu/cdm4/item_viewer.php?CISOROOT=/UU_EAD&amp;CISOPTR=160">http://content.lib.utah.edu/cdm4/item_viewer.php?CISOROOT=/UU_EAD&amp;CISOPTR=160</a>	432
	[13] Taubes 1993, p. 424.	433
	[14] Huizenga 1993, p. 184.	434
435	[15] Taubes 1993, pp. 136–138.	
436	[16] C. Rolfs and E. Somorjai, Nucl. Instrum. Methods B <b>99</b> , 297 (1995).	
437	[17] K. Czerski, A. Huke, P. Heide, M. Hoefl, and G. Ruprecht in <i>Nuclei in the Cosmos V, Proceedings of</i>	
438	<i>the International Symposium on Nuclear Astrophysics</i> , edited by N. Prantzos and S. Harissopulos	
439	(Editions Frontieres, Volos, Greece, 1998) p. 152.	
440	[18] K. Czerski, A. Huke, A. Biller, P. Heide, M. Hoefl, and G. Ruprecht, Europhys. Lett. <b>54</b> , 449 (2001).	
441	[19] A. Huke, Ph.D. thesis, Technische Universitat Berlin, 2002, <a href="http://edocs.tu-berlin.de/diss/2002/huke_armin.htm">http://edocs.tu-</a>	
442	<a href="http://edocs.tu-berlin.de/diss/2002/huke_armin.htm">berlin.de/diss/2002/huke_armin.htm</a> .	
443	[20] Japan C-F Research Society site	
444	[21] Japan CF research society meeting Dec 2011	
445	[22] Szpak, Masier-Boss: Thermal and nuclear aspects of the Pd/D2O system, Feb 2002. Reported by	
446	Mullins 2004	
447	[23] F. Raiola <i>et al.</i> , Eur. Phys. J. A <b>13</b> , 377 (2002);	
	[24] F. Raiola <i>et al.</i> , Phys. Lett. <b>B547</b> , 193 (2002).	448
449	[25] C. Bonomo <i>et al.</i> , Nucl. Phys. <b>A719</b> , 37c (2003).	
450	[26] F. Raiola <i>et al.</i> , Eur. Phys. J. <b>A 19</b> , 283 (2004).	
451	[27] A. Huke, K. Czerski, and P. Heide, Nucl. Phys. <b>A719</b> , 279c (2003).	
452	[28] P. Kalman and T. Keszthelyi, Phys. Rev. C <b>69</b> ,031606(R) (2004).	
453	[29] Mullins 2004	
	[30] Broad 1989b, Voss 1999, Platt 1998, Goodstein 1994, Van Noorden 2007, Beaudette 2002, Fedor	454
	2005, Adam 2005, Kruglinksi 2006, Adam 2005, Alfred 2009	455
	[31] Simon 2002, pp. 131–133,218	456

	[32] Seife 2008, pp. 154–155	457
	[33] Hubler 2007	458
	[34] Biberian 2007	459
460	[35] J. Kasagi <i>et al.</i> , J. Phys. Soc. Jpn. <b>71</b> , 2881 (2002)	
461	[36] K. Czernski <i>et al.</i> , Eurouphys. Lett. <b>54</b> , 449 (2001); Nucl. Instrum. Methods Phys. B <b>193</b> , 183 (2002).	
462	[37] A. Huke <i>et al.</i> , Phys. Rev. C <b>78</b> , 015803 (2008).	
463	[38] A. Huke, K. Czernski, S. M. Chun, A. Biller, and P. Heide, Eur. Phys. J. <b>A35</b> , 243 (2008).	
464	[39] P. Kalman and T. Keszthelyi, Phys. Rev. C <b>79</b> , 031602(R) (2009).	
465	[40] K. Hagino and A. B. Balantekin, Phys. Rev. C <b>66</b> , 055801 (2002).	
466	[41] S. Kimura <i>et al.</i> , Phys. Rev. C <b>67</b> , 022801 (2003).	
467	[42] G. Fiorentini <i>et al.</i> , Phys. Rev. C <b>67</b> , 014603 (2003).	
468	[43] J. H. Hamilton, <i>Internal Conversion Processes</i> (Academic, New York, 1966).	
469	[44] C. Angulo <i>et al.</i> , Nucl. Phys. <b>A656</b> , 3 (1999).	
470	[45] J. M. Ziman, <i>Principles of the Theory of Solids</i> (Cambridge University Press, Cambridge, 1964), pp.	
471	148-150 .	
472	[46] K. Alder <i>et al.</i> , Rev. Mod. Phys. <b>28</b> , 432 (1956).	
473		
474		
		475
476		